VOLTAGE CLAMP WITH DOUBLE SUCROSE GAP TECHNIQUE

External Series Resistance Compensation

J. P. POINDESSAULT, A. DUVAL, *and* C. LÉOTY

From the Laboratoire de Physiologie Animale, Faculté des Sciences, Université de Poitiers, 86022 Poitiers, France

ABSTRACT In this paper we deal with the double sucrose-gap voltage clamp technique. To perform a reliable clamp or to analyze the intracellular potential distribution, any external series resistance in the artificial node must be taken into account for it induces an instability in the external potential as soon as a current develops. A circuit was designed to compensate for this error, it has been found effective on an analog model and on experimental uni- or multicellular preparations. The attenuation in series resistance frequently causes ringing in the step response. This behavior was studied theoretically and also simulated with analog models where a selective bridged-T network was found to represent the electrical characteristics of the preparation when associated with the chamber and control electronics. A residual series resistance was found and is considered to be a part of the preparation. Characteristics necessary to obtain best results are proposed, for a preparation to be studied in experiments utilizing the double sucrose gap technique with external series resistance compensation.

INTRODUCTION

The double sucrose-gap voltage clamp technique has been widely used on different excitable tissues, but since Johnson and Lieberman (1971) first criticized its application to multicellular preparations, others (Harrington and Johnson, 1973; Tarr et al., 1973; Tarr and Trank, 1974; Ramõn et al., 1975) have become more skeptical about analysis of results, even with unicellular material (Moore et al., 1975). Experiments and computer simulations made by these authors show that the main limitations of the technique are (*a*) the cable properties of the studied segment, (*b*) the existence of a resistance in series with the membrane, and (*c*) the multicellular structure of some preparations.

In an attempt to measure the distribution of potential in multicellular and unicellular preparations, it was soon realized that such intracellular measurements were not reliable, since it was found that the external potential varied as a current developed. Some attempts to eliminate the series resistance have already been made by reducing the distance between the voltage reference electrode, in the central compartment, and the

preparation. Since in our experimental set-up such a modification did not lead to a sufficient improvement, a convenient electronic arrangement was designed.

The aim of the present paper is to evaluate the effectiveness of this circuit in experiments with both frog atrial and skeletal muscle preparations and to analyze the results obtained. This leads to a simple equivalent model for the whole system, including the chamber, the preparation and the control electronics, and it leads to the determination of what the optimal physical characteristics of a preparation should be if the double sucrose gap technique is used.

A preliminary report of the present results was published (Léoty and Poindessault, 1974).

METHODS

Voltage Clamp Electronics

The schematic diagram of the double sucrose gap chamber and the associated electronics used for voltage clamp experiments is given in Fig. 1A. The central compartment electrode C_1, which is intended to determine the potential at the outside of the preparation, is held at ground potential by the inverting input of the current-to-voltage converter (*IVC*), the output voltage of which (I_m) is proportional to the total current flowing into or out of the test compartment. The potential at the inside of the preparation is sensed by the inverting input of the control amplifier (*CA*), via the voltage pool electrode (*R*) and is compared to the command voltage (V_c) applied to the noninverting input. The feedback loop is closed through the preparation by connecting the current pool electrode (*L*) to the output of the control amplifier.

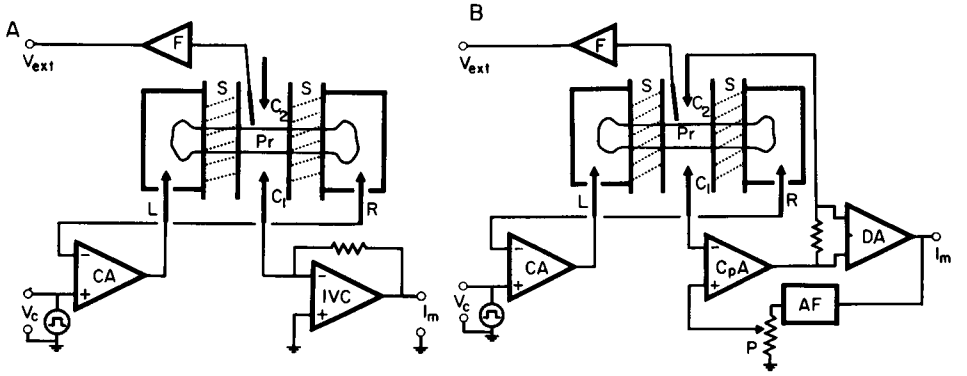

FIGURE 1 Schematic diagram of the experimental chamber and electronic set-up. *S*, sucrose channels; P_r, preparation; *L*, current pool electrode; C_1, C_2, central compartment electrodes; *R*, voltage pool electrode; V_c, command voltage; V_{ext}, external potential measurement; I_m membrane current measurement. (*A*) Basic voltage clamp circuit: *CA*, control amplifier (45K, Analog Devices, Inc., Norwood, Mass.); *IVC*, current to voltage converter (LH0042, National Semiconductor Corp., Santa Clara, Calif.); *F*, negative capacitance high input impedance amplifier (built with a NSC LH0042). (*B*) The circuit which compensates for the external series resistance is added: C_pA, compensation amplifier (uses a NSC LH0042 or Analog Devices AD 504K); *AF*, universal active filter (three LM 741); *P*, potentiometer which controls the restoration of equivalent series resistance; *DA*, differential amplifier (Analog Devices AD 520K).

In such a configuration, the external surface of the studied segment of membrane would be held at ground potential whereas the internal one follows the command voltage.

External Potential Measurements in the Test Compartment

With no external series resistance, the potential at the outside of the preparation would be that of electrode C_1, i.e. the ground potential. The deviations (V_{ext}) from this condition are monitored with respect to ground by an Ag-Ag-Cl electrode (20 μm in diameter) placed in close vicinity to the preparation in the test node and connected to an electrometer-input, negative capacitance amplifier (F). The same set-up could be used with KCl-filled microelectrodes for intracellular recording.

Circuit which Compensates for the Effects of the External Resistance in the Test Compartment

The purpose of this circuit is to cancel any current flow in the series resistance between the preparation and the voltage reference electrode C_1. Its schematic diagram is added to the basic voltage clamp circuit in Fig. 1B.

If the wiper of potentiometer P is at ground, the noninverting input of the compensation amplifier (C_pA) is at ground. Hence, as a feedback loop is built around this amplifier via C_2, the central compartment, and C_1, the inverting input (i.e. C_1) is a virtual ground and the voltage clamp circuit may operate as previously. Moreover, since no current can flow into or out the high impedance, low-input current, inverting input of the compensation amplifier, its output delivers (or sinks), via C_2, into (or from) the central compartment the current which would normally flow by C_1, i.e. the "membrane current." This prevents any RI drop between the preparation and C_1. The membrane current is measured as a voltage drop on a known resistance, inserted into the feedback loop, by a differential amplifier (DA) the output of which is a voltage (I_m) proportional to the current.

To recreate an equivalent series resistance in the test node, the reference electrode C_1 may be driven to a potential proportional to the membrane current. This is done with appropriate scaling by means of potentiometer P. A universal active filter (AF) allows the restoration of series resistance effects in a limited and shaped band of frequency.

Swept Frequency Measurements

In order to evaluate the frequency response of the overall system (preparation, chamber and control electronics) under voltage clamp conditions, either with or without series resistance compensation, a small amplitude (10 mV peak to peak), frequency-swept sine-wave is applied as command voltage V_c. This signal is generated by a HP 3310 A function generator (Hewlett-Packard, Palo Alto, Calif.) driven on its VCO input by a voltage ramp (0–10 V). The output of the control amplifier (CA), or that of the current measuring amplifier (DA), is displayed as the vertical signal on a memory oscilloscope (Tektronix 5115, Tektronix, Inc., Beaverton, Ore.) in XY mode with the sweeping ramp as the horizontal deflection. The peak-to-peak amplitude vs. frequency record is displayed with linear scales both on the vertical and horizontal axis.

Impedance Measurements (Voltage Clamp Circuit Disconnected)

The resistance between C_1 and C_2 is evaluated by applying a voltage step to C_2 and reading the current by means of a current-to-voltage converter connected to C_1. These two electrodes are placed symmetrically 1 cm apart from the central node. The resistance between the preparation and the voltage reference electrode C_1 is half of the measured resistance between C_1 and C_2. As the most part of the resistance is in the narrower part of the central path, its value is

insensitive to the small difference which may occur in the distance between the preparation and C_1 or C_2.

The longitudinal impedance of the preparation is measured by applying a reference voltage (step or variable frequency sine-wave) to the left electrode (L) and connecting the current-to-voltage converter to the right electrode (R).

Similarly, the impedance between the central compartment and lateral pools may be measured.

Electrodes

Electrodes L, R, C_1, and C_2 are all half-calomel electrodes. They were built to give much lower impedances, better stability and reproducibility than the Ag-Ag-Cl electrodes and agar-agar-bridges. Their impedance is essentially resistive (less than 50 Ω) and the difference in junction potential between any two of them is always less than 1 mV.

Chamber

Similar to that described by Rougier et al. (1968) the chamber was built entirely of Perspex. The width of each channel could be changed independently while the central compartment was designed to make the external series resistance as low as possible (7 KΩ between C_1 and C_2).

Preparations

The experiments were carried out on 45 atrial trabeculae (80–250 μm in diameter and 3–4 mm long) and on 30 single skeletal muscle fibers (semitendinosus, 50–100 μm in diameter and 2–3 cm long) isolated from the frog *Rana esculenta*. The tested segment (artificial node) was 40–100 μm long.

Solutions

The physiological solution had the following composition in millimoles per liter: NaCl, 110.5; KCl, 2.5; $CaCl_2$, 1.8; $NaHCO_3$, 2.4; the pH was adjusted to 7.3 or 7.8. The isotonic sucrose solution contained 214 mmol/liter. All experiments were performed at room temperature (18–20°C).

Computer Simulations

The computer simulations are performed on a Tektronix DPO fitted with a DEC PDP 11/05 (16 kilowords) and TEK BASIC V01-01. The model is a single patch Hodgkin-Huxley type, with added series resistance such as that used by Tarr et al. (1973) and is adapted to heart or skeletal muscle. The program (BACLA 7) runs in 4 min for 500 increments in time and outputs sodium conductance, sodium current, transmembrane potential, capacitive current, and total current. The early versions of BACLA were derived from a FORTRAN program published by Palti (1971).

RESULTS

Loss in Voltage Control Due to an External Series Resistance

In single cells from frog skeletal muscle or in frog atrial trabeculae, the current generated by an applied depolarization develops in a manner similar to that reported by Ildefonse and Rougier (1972) and Rougier et al. (1968) using the same method (Fig. 2 A, B, middle traces). A voltage drop simultaneous with the variation in membrane

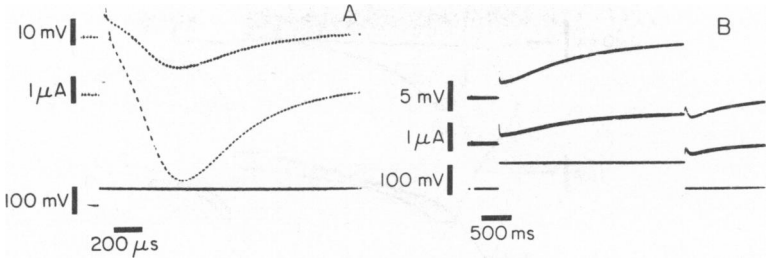

FIGURE 2 Simultaneous recording of the membrane current (middle traces) and the variation in the external potential (upper traces) induced by a depolarization (lower traces). (*A*) In a single skeletal muscle fiber for a short depolarization which induces the maximum fast inward current. (*B*) In an atrial trabecula for a long depolarizing step which generates outward current.

current is recorded with respect to ground in the liquid surrounding the preparation (Fig. 2 A, B, upper traces). For a given depolarization this variation in potential is proportional to the current intensity, i.e. $V_e = R_s \cdot I_m$, where V_e is the external potential, I_m the intensity of the recorded current, and R_s is defined as the external resistance in series with the preparation. This linear relationship is confirmed when the value of a known, added, series resistance is calculated from the external voltage and current records.

Those experiments, which confirm the simulations done by Ramõn et al. (1975), show, regardless of the particular preparation, how dramatic the loss in external voltage control can be, especially when the early inward current develops. It is important to notice that as soon as a current flows, whatever its kinetics or nature (i.e., fast inward, slow inward, delayed outward, or even steady state), there is a deviation from the theoretical ground potential required at the outside of the preparation. This loss in voltage control arises only from the *RI* drop on the external series resistance, and so must be considered even if the internal membrane potential is assumed to be homogeneous and closely follows the command step. Hence it appeared necessary to get fairly good control of the external potential before any attempt to study the intracellular potential distribution could be made.

Compensation of the Effects of the External Series Resistance

The superimposed records of Fig. 3 allow to compare actions of the current waveforms and the external potential variations when the compensating circuit is (*a*) or is not used (*b*). The loss in external potential control appears to be greatly reduced by the compensating circuit though the peak of the inward current is larger. A similar result has already been obtained on frog atrial tissue (Léoty and Poindessault, 1974). However, the lack of ringing shown by Fig. 3 (middle trace) is not always observed, as illustrated by the experiment in Fig. 4 A. Here, the fast inward current is inactivated by a change in the holding potential. The fact that the responses at the leading and trailing edge of the command step are identical shows that the ringing is only due to

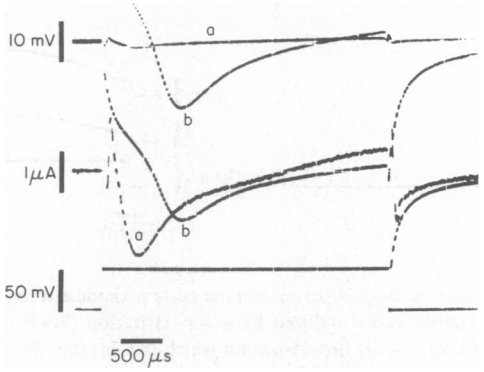

FIGURE 3 For a given depolarization (lower trace) effects of the series resistance compensation on the external potential (upper trace) and the membrane current (middle trace) records in a frog skeletal muscle fiber; *b*, in normal conditions; *a*, when the series resistance is compensated.

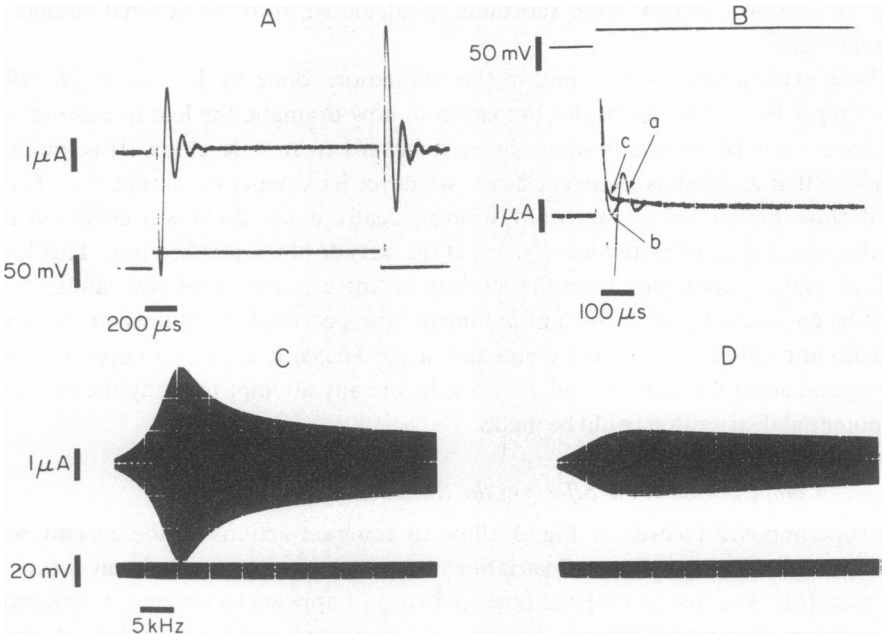

FIGURE 4 Step (*A*, *B*) and frequency (*C*, *D*) response recorded in the same frog skeletal muscle fiber. The holding potential is set to inactivate the fast inward current. *A* and *C*: the series resistance is fully compensated; *B*: an equivalent series resistance is progressively restored to be 1 KΩ (*a*), 5 KΩ (*b*), and 8 KΩ (*c*); this last value leads to a critically damped step response and the related frequency response is shown in *D*.

some passive properties of the whole system, including the preparation, the chamber, and the electronics.

To get more information on the behavior of the system, successive step response and frequency response measurements were done on a preparation. As the effectiveness of the compensation is decreased by restoring some known equivalent series resistance, the ringing is progressively and finally fully damped (Fig. 4 B) whereas the frequency response curve flattens (Fig. 4 C, D). Thus the system behaves like a second order, high pass, active filter; the damping ratio of which follows the series resistance variation. In these experiments, the ranges of the peak frequency were 500 Hz to 1.5 KHz for the frog atrial bundles and 5 KHz to 15 KHz for the skeletal fibers.

DISCUSSION

Voltage Clamp Data Interpretation and Series Resistance

The existence of an external series resistance in a double sucrose gap chamber has already been reported (Rougier et al., 1968; Tarr and Trank, 1971) but its effects have not yet been extensively described. We will outline here, only some problems arising from this technical point when interpreting voltage clamp data obtained, either on unicellular or multicellular preparations.

If one attempts to compare two currents, different in shape or amplitude, and recorded in experimental conditions where the voltage drop on the series resistance has not been completely eliminated, these currents have been, in fact, elicited by two different stimulating waveforms although the step command was the same. Under such conditions, the substraction method, performed with a hyperpolarizing pulse (Harrington and Johnson, 1973) or specific inhibitors (Rougier et al., 1968; Ildefonse and Roy, 1972; Mironneau, 1974) yields doubtful "net current" patterns. To illustrate this point, computer simulations have been done. Among the results shown in Fig. 5, the shape of the effective transmembrane potential (D) and the resultant capacitive current (C) have to be noticed.

Avoiding Series Resistance Effects

Two techniques have previously been used to avoid the problems due to the presence of a resistance in series with the studied membrane segment.

(*a*) An auxiliary electrode is placed as close as possible to the preparation in order to control the external potential more accurately (Julian et al., 1962; Tarr and Trank, 1971).

(*b*) A negative resistance is generated between the voltage control points (compensated feedback; Hodgkin et al., 1952).

The first technique can be implemented in two ways: (*1*) with an Ag-Ag-Cl electrode (Nakajima and Bastian, 1974; Tarr and Trank, 1971) which however cannot be placed in close contact with the whole surface of the preparation. It is probably still connected to it by a residual series resistance which may not be negligible since we found

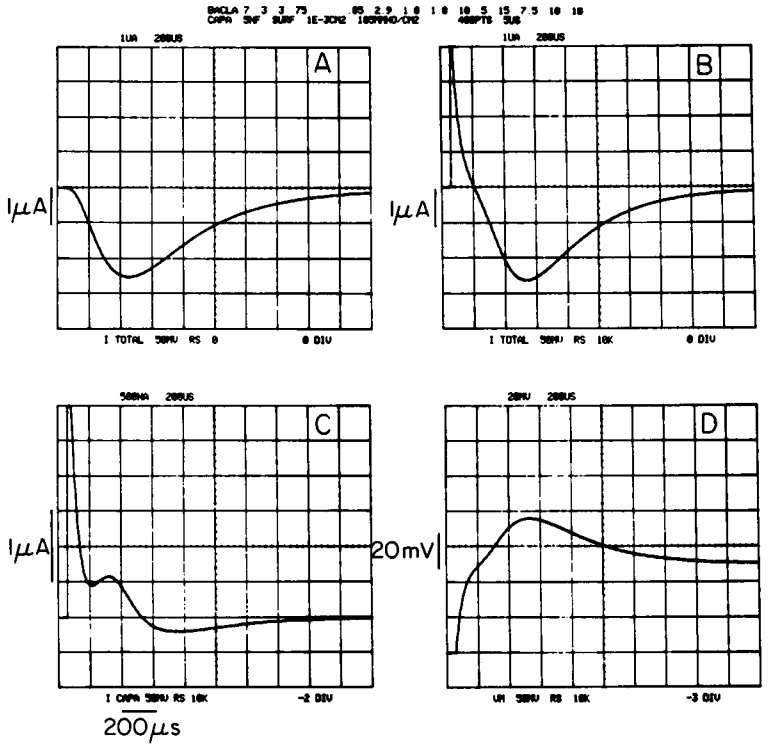

FIGURE 5 Simulation of the effective current and voltage patterns in a skeletal muscle fiber when the series resistance is not compensated. The stimulation is 50 mV. (*A*) For reference, membrane current in absence of the series resistance. (*B*) Membrane current for 10 KΩ of series resistance. (*C* and *D*) Respectively, corresponding capacitive current and transmembrane potential.

most of the series resistance located in the immediate vicinity of the preparation; (*2*) with a microelectrode which allows a more accurate positioning but presents the drawbacks of point voltage control and those of high impedance and stray capacitive coupling with the somewhat large voltages developed in the current pool.

The technique of compensated feedback was adapted to our experimental systems by connecting a current negative immitance converter (INIC) to the central compartment electrode in order to generate a negative resistance at this point. Although it effectively reduces the series resistance, the circuit was not found suitable, mainly because of the difficulty in external potential control and in frequency stabilizing the INIC because its input is connected to a complex, varying, and not well-defined impedance.

The compensating circuit was designed to be easily incorporated into our previous apparatus and was found to effectively cancel the external potential variations during current flow without causing frequency stability problems itself.

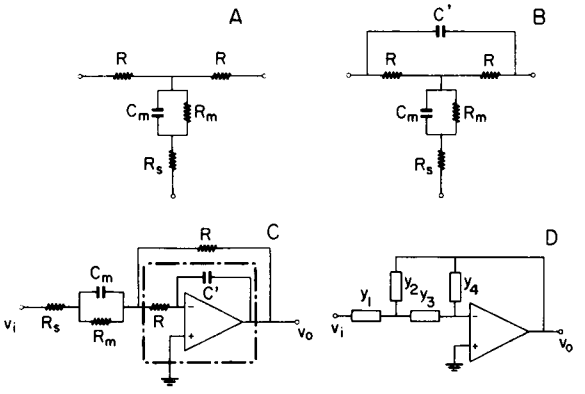

FIGURE 6 (*A*) Equivalent passive circuit of a preparation in a double sucrose-gap chamber including the series resistance. (*B*) Circuit modified to account for the selective frequency properties observed in experiments. (*C*) Connecting the circuit *B* to the amplifier reveals that the effective control amplifier is, in fact, an operational integrator (dashed-line box). (*D*) General diagram of a multiple feedback active filter. R, right and left part of the longitudinal intracellular impedance (assumed resistive); R_m, membrane resistance; C_m, membrane capacitance; R_s, series resistance; C', shunt capacitance between current and voltage pools.

Origin of the Ringing when the Series Resistance is Compensated

The second order response obtained when the series resistance is compensated results in the extension of the usual T model (Fig. 6 A) to a bridged-T network (Fig. 6 B) which exhibits a selective frequency response. This is done by including in the diagram the shunt capacitance C' which value may be as low as a few picofarads to explain the responses obtained on the various preparations used (see Appendix). Tests done with analog models showed that the electronic apparatus could not be responsible for this component. This capacity may result either from a stray coupling between the outer pools of the chamber or from a capacitive component in the longitudinal impedance of the preparation as reported by Freygang and Trautwein (1970) on Purkinje fibers and suggested by Tarr and Trank (1974) in frog atrial tissue. However, experiments done in the same chamber, both on frog atrial and skeletal muscle tissues, did not give significant variations in the value of C'. Thus this component seems to be a characteristic of the chamber rather than of the tissue. This does not necessarily deny the existence of a capacitive component in the intracellular longitudinal impedance since, as shown by Freygang and Trautwein (1970), it shunts only a small part of the overall resistance (17%) and is in series with the remaining part (at less 300 KΩ in our experiments).

Analysis of the Frequency Response Curves

Since the mathematical analysis of the response is given in the Appendix we will only outline here the general and most useful findings given by such an analysis.

(*a*) The drawing of the bridged-T network (Fig. 6 B) could be modified (Fig. 6 C) to show that, in fact, the control amplifier is an operational integrator resulting from the combination of the assumed ideal operational amplifier and integrating network (R, C'). The effective unity-gain frequency of the control amplifier (dashed-line box in Fig. 6 C) is thus dependent on the preparation and the chamber. In our chamber and with skeletal muscle fibers the best-case values are 1 pF for C' and 200 KΩ for R; they give an optimal unity-gain frequency near 800 KHz, leading to a too small open-loop gain of 38 dB (80) at 10 KHz when the series resistance is compensated.

The lower the intracellular longitudinal resistance and chamber stray capacitance are, the wider is the bandwidth of the effective control amplifier.

(*b*) The damping ratio is defined, on the frequency response curve, as the ratio of the −3 dB bandwidth to the peak frequency. Critical damping (giving the shortest capacitive current and no ringing) arises if the damping ratio η is equal to 0.7, ringing if η is less than 0.7 and overdamping if η is larger than 0.7.

If the series resistance is assumed to be fully compensated and the membrane resistance infinite, the damping ratio is: $\eta_o = (C'/C_m)^{1/2}$. The natural frequency of oscillation is: $f_o = 1/[2\pi R(C_m \cdot C')^{1/2}]$, where R is the assumed equal value for the right part and the left part of the intracellular pathway, C_m the membrane capacitance, and C' the stray capacitance between the outer pools.

If the ringing is kept at high frequency (such as 10 KHz for the frog atrial tissue and 50 KHz or more for skeletal muscle) and recovers quickly, it will not overlap the initial phase of the fast inward current. High frequency ringing may be achieved by decreasing first R and then C' and C_m, since they act by their square root. Fast recovery from ringing (or settling) implies a damping ratio as close as possible to 0.7, i.e. a low value for C_m since C' must be kept low as shown previously. Moreover, the amplitudes of the ringing peaks will decrease with C_m since they are related to the inverse of the damping ratio.

The results from the analysis of the particular case with R_s zero and R_m infinite may be extended to more real cases, where R_s is not zero, R_m finite, and, eventually, where a transverse tubular system equivalent branch is added to the model since the related damping ratio η may be expressed as a function of η_o.

In short, the best results under external series resistance compensation are achieved if (*1*) the stray capacitance between the outer pools of the chamber is made very low (less than 1 pF), (*2*) the intracellular longitudinal resistance is low (less than 100 KΩ), and (*3*) the membrane capacitance is low (about 1 μF/cm^2).

Although the first requirements may be met by appropriate screening (Nakajima and Bastian, 1974), the two others are quite contradictory, since an increase in the diameter of the preparation decreases the longitudinal resistance but increases the membrane capacitance of the tested segment. This may be compensated by reducing the test compartment width. Such a procedure will reduce the length-diameter ratio of the studied segment but an increase in the diameter of a multicellular preparation will probably lead to a reduced internal potential control.

Internal Series Resistance

The damping ratio computed from the frequency response curves obtained under full compensation is far from the values which would be expected if only the membrane capacitance and the stray capacitance are taken into account. For instance, from Fig. 4 C, the experimental damping ratio is 0.35 while the theoretical η_o would be 10 or more times less. The analog simulation of the experimental response leads one to consider the existence of a residual series resistance.

The record of Fig. 4 C was obtained on a single skeletal muscle fiber 100 μm in diameter with a 80 μm wide test node. The analog simulation of such a frequency response fits well with the experimental one if the values used for the model, deduced from the step response with uncompensated series resistance, are combined with a 1.8 KΩ residual series resistance and a 1.7 pF shunt capacitance. Similar experiments done with frog atrial bundles (200 μm in diameter and 100 μm wide test node) give a maximum residual series resistance of 3 KΩ. This value which is less than the mean 7.7 KΩ found by Tarr and Trank (1971) on the same preparation, seems to confirm that the external potential control effected by an auxiliary electrode close to the preparation does not satisfactorily solve the problem of the external series resistance. Moreover, this has to be considered when interpreting intracellular control data published by the same authors (Tarr and Trank, 1974).

The residual series resistance we found may be located either at the surface of the preparation (connective tissue in skeletal muscle fiber) or on the inside (extracellular paths in frog atrial bundles) or both. Considering the surface of the preparation as the surface of its cylindrical envelop, the residual series resistance is about 0.45 $\Omega \cdot cm^2$ for the skeletal muscle and 1.9 $\Omega \cdot cm^2$ for the frog atria. These values are less than or near the 2 $\Omega \cdot cm^2$ obtained on the axon by Hodgkin et al. (1952) with their compensating arrangement. Their value gave a damped step response and, combined with the low membrane capacitance of the axon, gave no noticeable lag in the early inward current development. Our values give underdamped step responses and, combined with the higher membrane capacitance of our preparations ($\times$ 200 for the atrial one), still give a significant lag in the rise of the transmembrane potential. Convenient damping would be achieved in skeletal muscle fibers if their intracellular longitudinal impedance was as low as that of the axon.

APPENDIX

The aim of the following frequency and step response study, on passive membrane equivalent models, is only to present as simply as possible the theoretical progression we have followed from the simplest (R_m; C_m) model to the bridged-T one deduced from the experiments reported in this paper. We will not give a complete analytical description of each response, just an outline of the influence of the model's component on the response.

The operational calculus is used and $f(p)$ would be the Laplace transform of $f(t)$:

$$L[f(t)] = f(p).$$

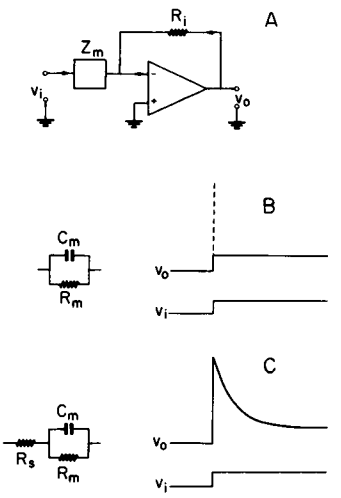

FIGURE 7 (*A*) Simplified voltage clamp equivalent circuit. Z_m is the membrane impedance and the series resistance, R_i is the feedback resistance equivalent to the longitudinal intracellular resistance between the current pool and the test node. (*B*) Step response of the parallel R_m; C_m equivalent circuit for Z_m. (*C*) Step response of the same circuit with added series resistance R_s.

Unless specified, the voltage clamp simplified equivalent circuit would be that of Fig. 7 A, the closed-loop gain of which is:

$$G_{cl} = v_o/v_i = -(R_i/Z_m). \tag{1}$$

v_i is the input voltage (sine-wave or step); v_o is the output voltage; R_i is the feedback path taken as the intracellular longitudinal resistance between the current pool and the test node; Z_m is the studied passive membrane equivalent model impedance. The operational amplifier is assumed to be ideal.

(1) Single Patch without Series Resistance

The impedance of the model of Fig. 7 B is given by:

$$1/Z_m = (1 + R_m C_m p)/R_m; \tag{2}$$

from Eq. 1 the closed-loop gain G_{cl} is:

$$G_{cl} = v_o/v_i = (1 + R_m C_m p)(R_i/R_m). \tag{3}$$

(*a*) the frequency response is that of a high-pass filter, the high frequency gain of which is non-limited (only limited in fact by the roll-off of the operational amplifier); (*b*) the response to a step of amplitude V, the Laplace transform of which is (V/p), is derived from Eq. 3:

$$v_o(p) = (V/p)(1 + R_m C_m p)(R_i/R_m). \tag{4}$$

Inverse transforming to the time domain gives:

$$v_o(t) = V(R_i/R_m) + L^{-1}(R_i C_m V), \tag{5}$$

where $L^{-1}(R_i C_m V)$ is the inverse transform of a constant, i.e. the impulse function (null width; surface $R_i C_m V$).

The step response of this elementary circuit is then the sum of its DC response and an impulse as represented on Fig. 7 B. Since the experimental results never show a response which can be confused with an impulse at time zero, the model is to be completed by adding a series resistance in order to stimulate the exponential decay of "capacitive" current, as shown in the following section.

(2) Single Patch with Series Resistance

The impedance of the model with series resistance (Fig. 7 C) is:

$$Z_m + R_s + R_m/(1 + R_m C_m p) \tag{6}$$

from Eq. 1 the closed-loop gain is:

$$G_{cl} = v_o/v_i = [R_i/(R_m + R_s)](1 + R_m C_m p)/\{1 + [R_m R_s/(R_m + R_s)]C_m p\}. \tag{7}$$

(a) the frequency response is deduced from Eq. 7. It has a zero at $f_{c1} = 1/2\pi R_m C_m$ and a pole at $f_{c2} = 1/2\pi[R_m R_s/(r_m + R_s)]C_m p$. The DC gain is $R_i/(R_m + R_s)$, the high frequency gain is limited at R_i/R_s. The voltage clamp system now behaves as a high-pass filter with finite gain in the pass-band. (b) the step response is given by:

$$v_o(t) = V[R_i/(R_m + R_s)][1 + (R_m/R_s)\exp(-t/\theta)] \tag{8}$$

where $\theta = [R_m R_s/(R_m + R_s)]C_m$ is the time constant of the exponential decay of "capacitive" current (Fig. 7 C).

This model simulates well the experimental response obtained when the external series resistance is not compensated.

(3) Single Patch with Compensated Series Resistance

Theoretically the response which can be expected when the external series resistance is compensated, would be that of the simplest (R_m; C_m) model without series resistance of section 1. However, though this model exhibits some ringing at high frequency (depending mainly on the frequency response of the operational amplifier), it cannot yield such low frequency ringing as that found with heart bundles. So, a model of the whole electrical path must be considered in order to simulate the experimentally observed selective frequency response. The most straightforward evolution of the previous models toward a selective network is the bridged-T of Fig. 6 B connected to the control operational amplifier (assumed ideal). The two parts of the longitudinal resistance are equal to the value R.

General Analysis. The circuit may be analyzed as the multiple-feedback active filter of Fig. 6 D where:

$$v_o/v_i = -Y_1 Y_3/[Y_4(Y_1 + Y_2 + Y_3) + Y_2 Y_3], \tag{9}$$

with:

$$Y_1 = (1 + R_m C_m p)/[(R_s + R_m) + R_s R_m C_m p],$$

$$Y_2 = 1/R = Y_3,$$

$$Y_4 = C' p.$$

The general Eq. 9 may be written as:

$$v_o/v_i = -RY_1/[R^2C'p(Y_1 + 2/R) + 1]. \quad (10)$$

Full Series Resistance Compensation: $R_s = 0$. For simplicity, R_m can be considered as infinite, so $Y_1 = C_m p$ and Eq. 10 gives:

$$(v_o/v_i)_0 = -RC_m p/(R^2C_mC'p^2 + 2RC'p + 1). \quad (11)$$

This response is that of a second-order high-pass filter of which the peaking in the frequency response and the ringing in the step response are related to the natural frequency: $f_o = 1/2\pi R(C'C_m)^{1/2}$, and to the damping ratio: $\eta_o = (C'/C_m)^{1/2}$.

Numerical example: With heart preparation, let $C_m = 0.15\ \mu$F and $R = 200$ KΩ; the stray capacitance, in our chamber, is: $C' = 1.5$ pF. From these values it is found that $f_o = 1{,}680$ Hz, and $\eta_o = 0.0032$. The value for f_o is in the range of experimental results but η_o is approximately 100 times less than the observed values.

This example shows that, if the relation giving f_o could be used with a rather good approximation,[1] the damping ratio must be increased with respect to η_o. This may be done by using in the model a capacitance (C_m) with series resistance (R_s) or with shunt resistance (R_m), or both.

Residual Series Resistance under Compensation: $R_s = R_{sr}$. R_m still being considered infinite, the admittance Y_1 is that of a capacitance C_m in series with a resistance R_{sr}:

$$Y_1 = C_m p/(1 + R_{sr}C_m p). \quad (12)$$

The general Eq. 10 becomes:

$$v_o/v_i = -RC_m p/[(R^2 + 2RR_{sr})C_mC'p^2 + (2RC' + R_{sr}C_m)p + 1]. \quad (13)$$

The natural frequency of oscillation is $f = 1/2\pi\sqrt{(R^2 + 2RR_{sr})C_mC'}$ and the damping ratio is $\eta = \eta_o[(1 + R_{sr}C_m/2RC')/\sqrt{1 + 2R_{sr}/R}]$. The coefficient of η_o may be simplified by series expansion and approximated to its first order term since higher order terms include the ratio (R_{sr}/R) which is generally less than (1/100). It comes:

$$\eta \simeq \eta_o[1 - (R_{sr}/R)(1 - C_m/2C')],$$

and since $C_m \gg C'$, 1 may be neglected with respect to $(C_m/2C')$; then:

$$\eta \simeq \eta_o[1 + (R_{sr}/2R)(C_m/C')]. \quad (14)$$

By taking into account a residual series resistance when the compensation circuit is used, the damping ratio is increased to more realistic values while the natural frequency of oscillation is slightly lowered.

Numerical example: The values of the previous example are used: $C_m = 0.15\ \mu$F; $R = 200$ KΩ; $C' = 1.5$ pF and the residual series resistance is given by the average value found in experiments: $R_{sr} = 2{,}000\ \Omega$. This leads to: $f = 1{,}660$ Hz and $\eta \simeq 1.6$. Since the damping ratio is larger than 0.7 the step response is overdamped as it is frequently observed with heart preparations.

In order to compare these results with the response in skeletal muscle fibers, the membrane capacitance is changed and give a value near that found in the experiment shown in Fig. 4:

[1] The natural frequency (f_n) is not strictly the frequency of the ringing (f_r) which is related to it by: $f_r = f_n(1 - \eta^2)^{1/2}$.

C_m = 0.003 μF. The natural frequency of oscillation is: f = 11.7 KHz, and the damping ratio becomes: $\eta \simeq 0.246$. This response is underdamped ($\eta < 0.7$) and would be close to the experimental one (f = 10.5 KHz; η = 0.35) if the transverse tubular system was taken into account in the model, since this component was found to add some more damping in the response.

These examples show that the inclusion of a residual series resistance in the model may lead to an analytical description which agrees well with the experimental results. However before discussing the reliability of this result, the influence of the membrane resistance must be defined.

Role of the Membrane Resistance. The role of the membrane resistance in the frequency and step response, when the compensation circuit is used, is studied with R_m finite and the series resistance R_s zero. In general Eq. 10, Y_1 is now the admittance of capacitance C_m shunted by resistance R_m,

$$R_m = Y_1 = (1/R_m)(1 + R_m C_m p).$$

Then Eq. 10 is:

$$v_o/v_i = -(R/R_m)(1 + R_m C_m p)/[R^2 C_m C' p^2 + (R^2/R_m + 2R)C'_p + 1] \qquad (15)$$

The natural frequency of oscillation is yet $f_o = 1/2\pi R\sqrt{C_m C'}$ and the damping ratio is $\eta = \eta_o[1 + (R/2R_m)]$. So, taking R_m finite does not modify the natural frequency but increases the damping ratio. The following numerical application will show whether or not this is an influence experimentally.

Numerical example: The values are that of the section on full series resistance compensation: C_m = 0.15 μF; R = 200 KΩ; C' = 1.5 pF, and to be demonstrative half of the average experimental R_m is used, R_m = 50 KΩ. The natural frequency is still f_o = 1,680 Hz, and the damping ratio is $\eta = 3\ \eta_o \simeq 0.01$. This value does not agree with the experimental results despite the low R_m, thus it may be concluded that practical values for R_m do not contribute much to the characteristics of the response.

Conclusion

The frequency and step response of both heart and skeletal muscle preparations are described analytically for experiments performed with the double sucrose-gap technique and with external series resistance compensating circuit. The main electrical parameters involved in the response of the whole system are the membrane capacitance, the intracellular longitudinal resistance, the stray capacitance lying between the current and the voltage pools, and to a lesser extent, the transverse tubular system impedance for the skeletal muscle fibers. Our analysis is valid as long as the high-frequency limiting element is the low pass-filter including the intracellular longitudinal resistance between the test node and the voltage pool (R_r) and the stray capacitance between the current and voltage pools (C'). Thus, the control amplifier must have a 20 dB/decade frequency roll-off and a unity-gain frequency (f_u) to that $f_u > 1/2\pi R \cdot C'$.

We wish to thank Doctors J. M. Kootsey and M. Lieberman for critically reading the manuscript, and Ms. P. Régondaud for her assistance.

This work was supported by Centre National de la Recherche Scientifique, Research Association Team no. 111, and performed under the Institut National de la Santé et de la Recherche Médicale (INSERM) grant A.T.P. no. 17.75.40.

Received for publication 28 April 1975.

REFERENCES

FREYGANG, W. H., and W. TRAUTWEIN. 1970. The structural implications of the linear electrical properties of cardiac Purkinje strands. *J. Gen. Physiol.* **55**:524.

HARRINGTON, L., and E. A. JOHNSON. 1973. Voltage clamp of cardiac muscle in a double sucrose gap. A feasibility study. *Biophys. J.* **13**:626.

HODGKIN, A. L., A. F. HUXLEY, and B. KATZ. 1952. Measurement of current-voltage relations in the membrane of the giant axon of *Loligo*. *J. Physiol. (Lond.).* **116**:424.

ILDEFONSE, M., and O. ROUGIER. 1972. Voltage-clamp analysis of the early current in frog skeletal muscle fibre using the double sucrose-gap method. *J. Physiol. (Lond.).* **222**:373.

ILDEFONSE, M., and G. ROY. 1972. Kinetic properties of the sodium current in striated muscle fibres on the basis of the Hodgkin-Huxley theory. *J. Physiol. (Lond.).* **227**:419.

JOHNSON, E. A., and M. LIEBERMAN. 1971. Heart: excitation and contraction. *Annu. Rev. Physiol.* **33**:479.

JULIAN, F. J., J. W. MOORE, and D. E. GOLDMAN. 1962. Current-voltage relations in the lobster giant axon membrane under voltage clamp conditions. *J. Gen. Pysiol.* **45**:1217.

LÉOTY, C., and J. P. POINDESSAULT. 1974. Effects and compensation of the series resistance in voltage clamp experiments using double sucrose gap technique. *J. Physiol. (Lond.).* **239**:108P.

MIRONNEAU, J. 1974. Voltage clamp analysis of the ionic currents in uterine smooth muscle using the double sucrose gap method. *Pfluegers Arch. Gesamte Physiol.* **352**:197.

MOORE, J. W., F. RAMON, and R. W. JOYNER. 1975. Axon voltage clamp simulations. II. Double sucrose-gap method. *Biophys. J.* **15**:25.

NAKAJIMA, S., and J. BASTIAN. 1974. Double sucrose-gap method applied to single muscle fiber of *Xenopus laevis*. *J. Gen. Physiol.* **63**:235.

PALTI, Y. 1971. *In* Biophysics and Physiology of Excitable Membranes. W. D. Adelman, editor. Van Nostrand-Reinhold Co., New York. Chap. 7.

RAMON, F., N. ANDERSON, R. W. JOYNER, and J. W. MOORE. 1975. Axon voltage-clamp simulations. IV. A multicellular preparation. *Biophys. J.* **15**:55.

ROUGIER, O., G. VASSORT, and R. STÄMPFLI. 1968. Voltage clamp experiments on frog atrial heart muscle fibres with the double sucrose gap technique. *Pfluegers Arch. Gesamte Physiol.* **310**:91.

TARR, M., E. F. LUCKSTEAD, P. A. JUREWICZ, and H. G. HAAS. 1973. Effect of propranolol on the fast inward sodium current in frog atrial muscle. *J. Pharmacol. Exp. Ther.* **184**:599.

TARR, M., and J. TRANK. 1971. Equivalent circuit of frog atrial tissue as determined by voltage clamp: unclamp experiments. *J. Gen. Physiol.* **58**:511.

TARR, M., and J. W. TRANK. 1974. An assessment of the double sucrose-gap voltage clamp technique as applied to frog atrial muscle. *Biophys. J.* **14**:627.